View Article Online / Journal Homepage / Table of Contents for this issue
Dynamic Article Links

Journal of
Materials Chemistry

Cite this: *J. Mater. Chem.*, 2012, **22**, 8394

www.rsc.org/materials

PAPER

Published on 15 March 2012. Downloaded by McMaster University on 29/10/2014 16:02:58.

Synthesis of diphenyl-diacetylene-based nematic liquid crystals and their high birefringence properties†

Yuki Arakawa, Shunpei Nakajima, Ryohei Ishige, Makoto Uchimura, Sungmin Kang,* Gen-ichi Konishi* and Junji Watanabe*

Received 19th November 2011, Accepted 13th February 2012
DOI: 10.1039/c2jm16002a

We synthesized two series of diphenyl-diacetylene (DPDA)-based materials with alkoxy and alkyl tails of length *m* (DPDA–OC*m* and DPDA–C*m*, respectively), and measured their nematic-phase birefringence (Δn) as a function of wavelength and temperature. We found that Δn decreases with an increase in *m*, possibly by a dilution effect of the low-Δn alkyl tail. Further, of the two series, Δn was found to be relatively higher in the DPDA–OC*m* materials, with the highest value of 0.4 obtained for DPDA–OC1 at 550 nm at 10 °C below the isotropic-to-nematic transition temperature. Further, we observed the temperature dependence for Δn, which is proportional to the order parameter (s). From extrapolation to $s = 1$ (the perfect orientation state), it is speculated that the DPDA–O moiety has the potential to afford a very large Δn of 0.9.

Introduction

With the strong commercial demand for flat panel displays and high-speed telecommunication devices, the applications of high-birefringence (Δn) liquid crystals (LCs) have extended to optical phase difference films, laser emission films and optical rotation plates. In these applications, such high-Δn materials offer the critical advantage of allowing smaller cell gaps and film thicknesses.

The preferred candidates for high-Δn LCs are compounds containing a conjugation along the long molecular axis.[1–13] Moreover, the presence of an acetylene unit (–C≡C–) is extremely effective as its Δn is approximately identical to that of phenyl groups. Thus, in the pursuit of high Δn, a range of LC molecules containing tolane, bistolane, diphenyl-diacetylene, and thiophenyl-diacetylene moieties[1–3,5–7,11–15] have been prepared thus far. In particular, Wu *et al.* reported that diphenyl-diacetylene with alkyl tails having carbon numbers *m* of 3–5 exhibited high Δn and low viscosity.[5,6] Other synthesized homologues of diphenyl-diacetylene with alkoxy, esters and fluorine groups have also been reported.[1–3,11,16–20] However, to our knowledge, their optical properties have not been investigated in detail, except for the materials prepared by Wu *et al.*[5,6]

In this study, we synthesized two series of diphenyl-diacetylenes with *p*-alkoxy tails ($m = 1$–7) and *p*-alkyl tails ($m = 4$–12) which form enantiotropic nematic LCs. Their birefringence Δn in the nematic phase was well elucidated as a function of *m*, wavelength, and temperature. Our results will be helpful in the design of final target polymers for application to optical phase difference films, laser emission films and optical rotation plates.

Experimental

Instruments

The ^{1}H NMR and ^{13}C NMR spectra were measured in $CDCl_3$ on a JEOL LNM-EX 400 at room temperature using tetramethylsilane (TMS) as an internal standard. The transition behavior was investigated by polarizing optical microscopy (POM) (Leica DM2500P microscopy with a Mettler FP90 hot stage) and differential scanning calorimetry (Perkin Elmer DSC7) with heating and cooling scans performed at 10 °C min^{-1}.

Materials

Unless otherwise noted, all chemicals were commercially available and used as received. Trimethylsilylacetylene, 4-iodophenol, $Pd(PPh_3)_4$, 4-bromoanisole (1-OC1) and 4-bromophenetole (1-OC2) (TCI), and alkyl bromide, PPh_3, CuI, 1,8-diazabicyclo [5,4,0]-7-undecene (DBU) and *N*,*N*,*N*′,*N*′-tetramethylethylenediamine (TMEDA) (Wako), and CuCl (Nacalai tesque) were purchased, respectively. 1,4-Bis(4-hexyloxyphenyl)buta-1,3-diynes were prepared according to Scheme 1. The chemical structures of 1-iodo-4-hexyloxybenzene (1-OC6),[21] 1-hexyloxy-4-[2-(trimethylsilyl)ethynyl]benzene (2-OC6),[22] and 1-ethynyl-4-hexyloxybenzene (3-OC6)[22] were confirmed by comparison with the corresponding literature. Our procedures for their synthesis are cited in the ESI†. Other compounds (DPDA–OC1–7) were synthesized in a similar manner as BPDA-OC6.

Department of Organic and Polymeric Materials, Tokyo Institute of Technology, 2-12-1 O-okayama, Meguro-ku, Tokyo 152-8552, Japan. E-mail: jwatanab@polymer.titech.ac.jp; konishi.g.aa@m.titech.ac.jp; skang@polymer.titech.ac.jp; Fax: +81 3-5734-2888; Tel: +81 3-5734-2321

† Electronic supplementary information (ESI) available: Typical DCS chart and spectral data. See DOI: 10.1039/c2jm16002a

This journal is © The Royal Society of Chemistry 2012

View Article Online

Published on 15 March 2012. Downloaded by McMaster University on 29/10/2014 16:02:58.

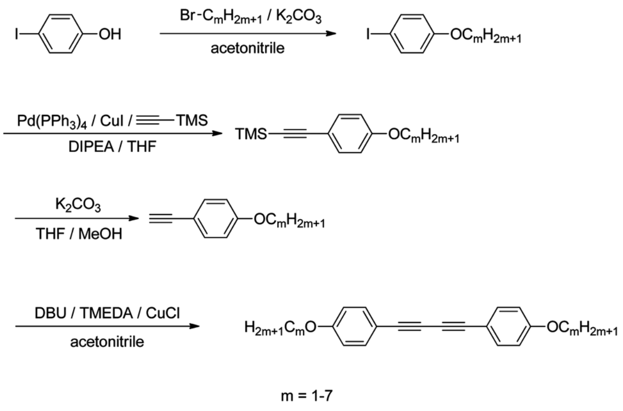

Scheme 1 Synthesis of dialkoxy-diphenyldiacetylene (DPDA–OC*m*).

1,4-Bis(4-hexyloxyphenyl)buta-1,3-diyne (4-OC6)

DBU (0.52 mL, 3.5 mmol), TMEDA (7.0 μL, 0.052 mmol), CuCl (6.9 mg, 0.07 mmol) and acetonitrile (10 mL) were bubbled with oxygen for 5 min, then 4-ethynyl-1-hexyloxybenzene (0.7 g, 3.5 mmol) was added to the mixture. The reaction was stirred at room temperature for 3 h. The solvent was removed under reduced pressure, and the obtained residue was extracted with diethylether, washed with water and dried over $MgSO_4$. After removing the solvent under reduced pressure and purifying by silica gel column chromatography (eluent: hexane), recrystallization with methanol was carried out to give **4-OC6** as a colorless solid (0.65 g, 93%). ^{1}H NMR (400 MHz, $CDCl_3$) δ 7.44 (d, J = 9.0 Hz, Ar–H, 4H), 6.84 (d, J = 9.0 Hz, Ar–H, 4H), 3.96 (t, J = 6.6 Hz, Ar–O–CH$_2$, 4H), 1.78 (tt, J = 6.6, 7.6 Hz, CH$_2$, 4H), 1.50–1.31 (m, CH$_2$, 12H), 0.91 (t, J = 7.1 Hz, CH$_3$, 6H) ppm. HRMS-DART (*m*/*z*): [M] calcd for $C_{28}H_{34}O_2$, 402.2558; found, 402.2559.

Results and discussion

Synthesis and characterization

As shown in Scheme 1, the synthetic route to dialkoxy-diphenyldiacetylene (DPDA–OC*m*) began with the synthesis of 4-alkyloxy-1-iodobenzenes with m = 1–7 by the Williamson ether reaction. Subsequently, 4-alkyloxy-1-ethynylbenzenes were prepared by palladium-catalyzed Sonogashira coupling, followed by base-induced hydrolysis.

Finally, 1,4-bis(4-alkoxyphenyl-1-yl)buta-1,3-diynes were obtained by Glaser coupling. The structures of the obtained compounds were confirmed by ^{1}H-NMR spectroscopy (see ESI†).

DPDA–C*m* (m = 4–12) were synthesized from 4-alkyl-1-ethynylbenzenes *via* a similar route.

Thermal properties

The thermal behaviors of DPDA–OC*m* (m = 1–7) and DPDA–C*m* (m = 4–12) were investigated by polarizing optical microscopy (POM) and differential scanning calorimetry (DSC). The representative DSC curves are shown in Fig. S1†, and the phase transition temperatures and enthalpy changes measured during the cooling scan are listed in Table 1. All the compounds exhibit an enantiotropic nematic phase.[2,5,6]

When the transition temperatures, T_i (isotropic to nematic) and T_c (nematic to crystalline), are plotted against m (Fig. 1), we can see at a glance that the LC temperature region of the DPDA–OC*m* series is higher than that of the DPDA–C*m* series. This is due to the dipolar interaction of the ether linkage. Further, as expected, the transition temperatures oscillate with even/odd m for both series. In DPDA–C*m*, the transition temperatures for odd-m members are higher than those for even-m members, whereas the DPDA–O*m* series exhibits the opposite trend; this opposite trend is due to the additional oxygen atom in the ether linkage.

The distinct feature in the LC behaviour of these materials is that the nematic phase formation is maintained when m is increased. This trend is in contrast to that in conventional materials, in which the nematic phase usually changes into the smectic phase because of the micro-segregation of the aromatic and aliphatic components. This obstinate nematic LC formation may stem from the good miscibility of the DPDA mesogenic moiety and the aliphatic tail.

Table 1 Phase transition temperatures (°C) and enthalpies (ΔH, kJ mol^{-1}) for DPDA–OC*m* and DPDA–C*m* obtained from cooling DSC thermograms at a rate of 10 °C min^{-1}

Material	Transition temperature/°C (enthalpy/kJ mol^{-1})
DPDA–OC1	Cr 98.6 (*23.8*) N 183.6 (*1.65*) Iso T_m: 141.9
DPDA–OC2	Cr 187.3 (*40.8*) N 208.8 (*1.66*) Iso T_m: 192.0
DPDA–OC3	Cr 123.4 (*17.5*) N 175.2 (*1.69*) Iso T_m: 139.5
DPDA–OC4	Cr 149.3 (*42.7*) N 173.6 (*2.26*) Iso T_m: 157.5
DPDA–OC5	Cr 110.1 (*33.3*) N 153.1 (*1.90*) Iso T_m: 119.1
DPDA–OC6	Cr 115.3 (*41.8*) N 147.5 (*2.01*) Iso T_m: 123.5
DPDA–OC7	Cr 92.7 (*23.7*) N 134.6 (*1.71*) Iso T_m: 104.6
DPDA–C4	Cr 65.1 (*12.8*) N 96.6 (*0.80*) Iso T_m: 76.3
DPDA–C5	Cr 79.0 (*11.5*) N 105.6 (*0.79*) Iso T_m: 86.2
DPDA–C6	Cr 55.3 (*20.5*) N 84.8 (*0.74*) Iso T_m: 60.1
DPDA–C7	Cr 81.0 (*20.6*) N 87.1 (*1.24*) Iso T_m: 89.7
DPDA–C8	Cr 59.0 (*18.2*) N 74.9 (*1.08*) Iso T_m: 66.3
DPDA–C9	Cr 69.6 (*20.1*) N 73.1 (*0.44*) Iso T_m: 78.5
DPDA–C10	Cr 51.5 (*24.9*) N 74.8 (*1.59*) Iso T_m: 57.7
DPDA–C12	Cr 57.3 (*5.45*) N 67.5 (*2.21*) Iso T_m: 62.8

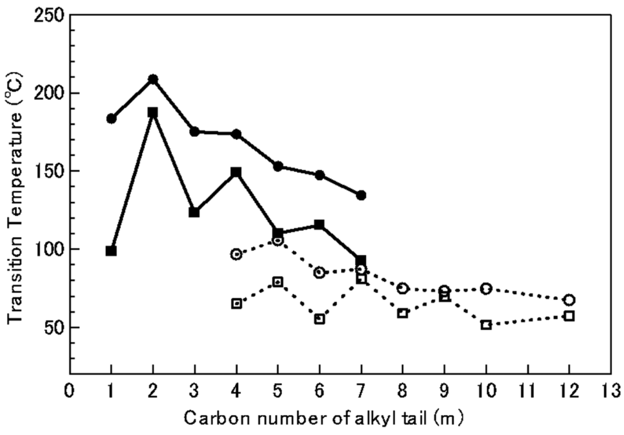

Fig. 1 Transition temperatures plotted as a function of the carbon number m of the alkyl tail in DPDA–OC*m* (closed symbols) and DPDA–C*m* (open symbols). The circles and squares are T_i and T_c, respectively.

Published on 15 March 2012. Downloaded by McMaster University on 29/10/2014 16:02:58.

The typical UV-vis spectra for DPDA–OC6 and DPDA–C6 (Fig. 2) show no dependence on *m*. Further, it can be observed that the longest absorption edges of the DPDA–C*m* and DPDA–OC*m* series are at 340 nm and 350 nm, respectively. This indicates that the DPDA moiety is an appropriate mesogenic unit since it is transparent in the visible wavelengths.[5,6]

Wavelength dependence of birefringence

In much of the literature,[1,2,7–10] the reported Δn values for high-Δn candidates are not actual measurements but extrapolations of values measured in a mixture with nematic LC compounds such as 5CB, *etc.* However, here, we measured actual values for the nematic LCs of pure target compounds.

The Δn measurement was performed for a homogeneously aligned nematic LC kept in a thin cell. Nematic alignment was achieved *via* the conventional method in which the nematic LC was sandwiched between two polyimide-coated glass plates that were rubbed to promote a homogeneous molecular orientation. The cell gap (4–6 μm) was precisely determined by the interferometric method. After filling the cell with the LC material, perfect alignment was confirmed under a polarized microscope. The transmittance of light under cross-polarization conditions was then observed as a function of wavelength by a microscope spectroscopic method using a Nikon LV100 Pol optical microscope equipped with a USB4000 (Ocean photonics) spectrometer. The transmitted light intensity I was modeled with the following equation:

$$I = I_0 \sin^2\left(\frac{\pi \Delta n d}{\lambda}\right)\sin^2\theta \tag{1}$$

$$\Delta n = a + \frac{b}{\lambda^2} + \frac{c}{\lambda^4} \tag{2}$$

where I_0, d, λ and θ represent the light intensity without a cell, cell thickness, wavelength and angle between extraordinary axis and polarization direction, respectively. Then, the observed transmittance was fitted with the calculated value by adopting Cauchy's equation (eqn (2)) for the wavelength dependence of Δn.

The measured values (Fig. 3) were successfully fitted with the theoretical curve fitting, which allowed the determination of the wavelength dependence of Δn.

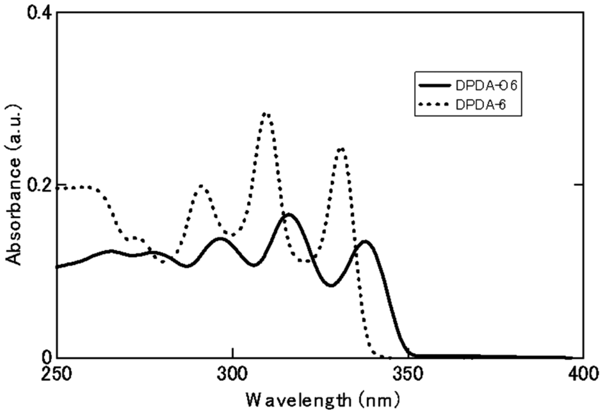

Fig. 2 UV-vis absorption spectra of DPDA–OC6 (solid curve) and DPDA–C6 (dashed curve) in THF.

The Δn values of the standard 5CB material and DPDA–C5 measured here (see Fig. 4a) correspond to those reported in the literature,[5,23] which supports the credibility of our measurement. All the compounds exhibited higher Δn than 5CB, which is attributable to the long conjugated DPDA. Further, the birefringence of DPDA–OC*m* is relatively higher than that of

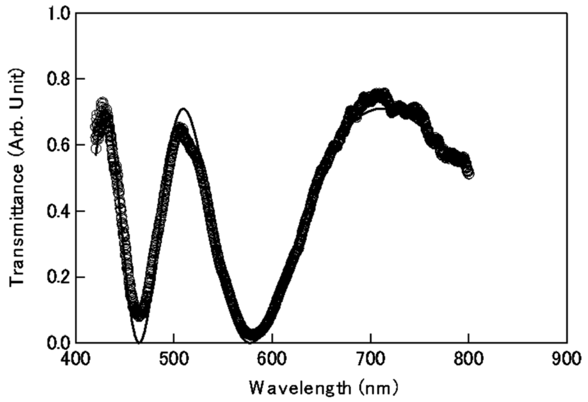

Fig. 3 Wavelength dependence of light intensity (open circles) transmitted through a homogeneous nematic cell of DPDA–OC1 under cross-polarization conditions. Here, the orientation direction of the nematic phase was set at 45° to the polarization axis. The solid curve is the fitting of eqn (1).

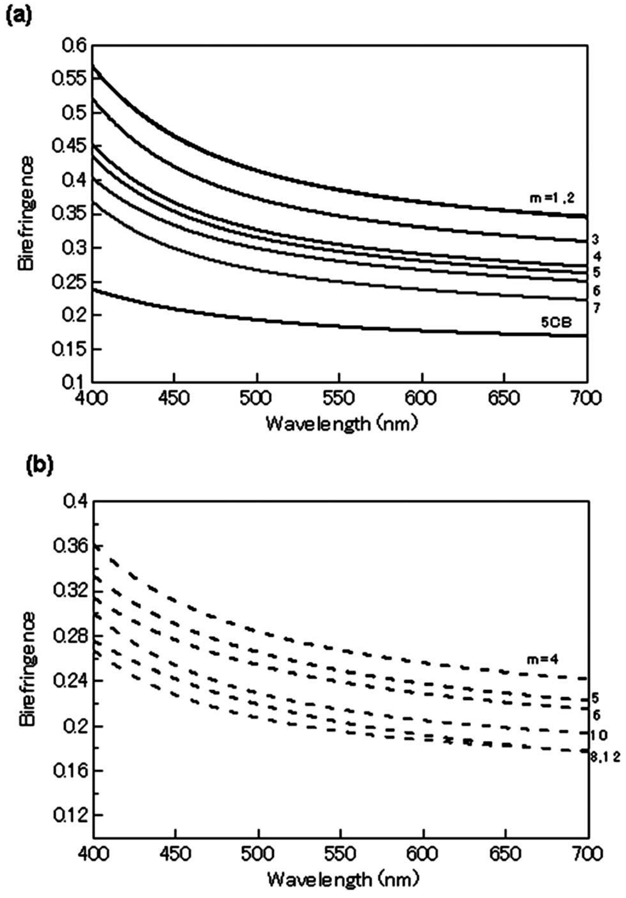

Fig. 4 Birefringence dispersion in the (a) DPDA–OC*m* and (b) DPDA–C*m* series. The birefringence measurements were performed at temperatures 10 °C below T_i.

This journal is © The Royal Society of Chemistry 2012

Published on 15 March 2012. Downloaded by McMaster University on 29/10/2014 16:02:58.

DPDA–C*m* because of the longer conjugation afforded by the coupling of the ether oxygen with the DPDA core.

Fig. 4a and b further demonstrate that when m is increased, Δn reduces in both systems. This trend is more remarkable in DPDA–OC*m* at lower m. Several reasons are considered: the dilution effect,[24] order parameter effect,[25] and decreased optical anisotropy.[24] The analysis shown later will indicate that the reduction is produced by the dilution effect by the alkyl tails, which do not contribute to the molecular polarizability as effectively as the mesogen. Thus, it is concluded that DPDA–OC1, with shortest tail, exhibits the highest Δn of 0.4 at 550 nm, making it a candidate high-Δn material.

Temperature effect

The value of Δn is proportional to the order parameter s,

$$\Delta n = \Delta n_0 s \tag{3}$$

and s depends on the temperature as,[26]

$$s = (1 - T/T_{\mathrm{i}})^{\beta} \tag{4}$$

Then, the temperature dependence of Δn is given by

$$\Delta n = \Delta n_0\,(1 - T/T_{\mathrm{i}})^{\beta} \tag{5}$$

Here Δn_0 is the birefringence for the nematic LC perfectly oriented ($s = 1$), and β is a constant that is characteristic of the nematic material.

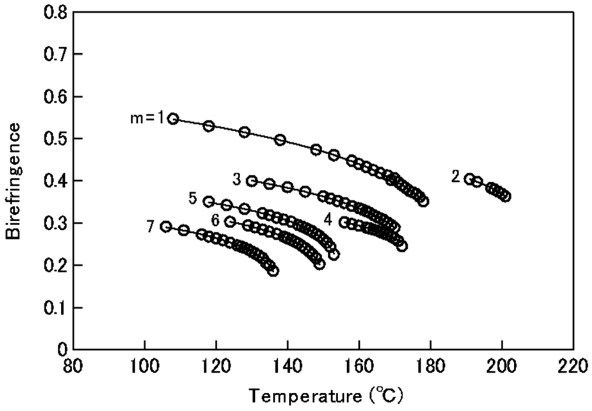

Fig. 5 Temperature dependence of birefringence (open circles) measured at a wavelength of 550 nm for DPDA–OC*m*. The solid curves are the fittings of eqn (5).

Table 2 Values of Δn_0 and β in eqn (5) estimated by curve fitting for DPDA–OC*m*

Material	Δn_0	β
DPDA–OC1	0.77	0.20
DPDA–OC2	0.68	0.17
DPDA–OC3	0.60	0.18
DPDA–OC4 (eqn (6))	0.55	0.15
DPDA–OC5	0.50	0.15
DPDA–OC6	0.46	0.16
DPDA–OC7	0.44	0.16

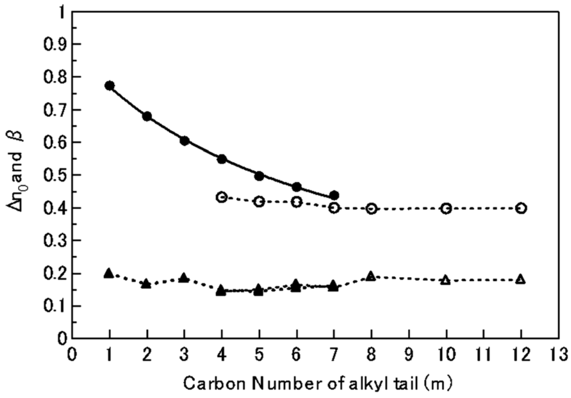

Fig. 6 Plot of n_0 (circles) and β (triangles) from eqn (6) determined by fitting against the carbon number m of the alkyl tail in DPDA–OC*m* and DPDA–C*m*. The solid curve for the values of Δn_0 in DPDA–OC*m* is the fitting of eqn (6).

The temperature dependence of Δn was examined at 550 nm, as shown for DPDA–OC*m* in Fig. 5. In all the compounds, the fitting is very good, with the determined values of Δn_0 and β listed in Table 2. Further, by plotting Δn_0 and β against m (Fig. 6), we see an obvious increase in Δn_0 with a decrease in m but an almost constant β of around 0.2. The value of Δn_0 expected for the DPDA moiety that corresponds to the extrapolated value for $m = 0$ was found to be extremely large, about 0.9 at 550 nm.

The decrease in Δn with an increase in m can be explained by the dilution effect of the alkyl tail, since the contribution of the alkyl tail group to Δn is relatively small or negligible in comparison with that of the O–DPDA–O moiety. Indeed, it is probably less than 0.1 in the LC system. Thus, the Δn value can be approximated as

$$\Delta n = (\Delta n_1 + 2mv\,\Delta n_2)/(1 + 2mv) \approx 0.9/(1 + 2mv) \tag{6}$$

here, v is the ratio of the molar volume of methylene units in the alkyl tail to that of the O–DPDA–O moiety; and Δn_1 and Δn_2 are the birefringence values expected for the mesogenic moiety and alkyl tail part, respectively. The best fitting is attained when $v = 0.077$, as seen in Fig. 6. This volume ratio may be reasonable, since it is nearly equal to the weight ratio of 0.06.

Conclusions

We synthesized two series of DPDA-based LCs, DPDA–OC*m* (m = 1–7) and DPDA–C*m* (m = 4–12), and measured their nematic-phase birefringence as a function of the wavelength and temperature. The birefringence of the nematic LCs decreases with an increase in the alkyl tail length, which is considered to be the result of a dilution effect caused by the low-birefringent alkyl tail. Further, of the two series, the DPDA–OC*m* materials exhibited higher birefringence, with the highest value of 0.4 obtained for DPDA–OC1 at 550 nm at 10 °C below T_{i}. The birefringence, which is proportional to the order parameter s, depends significantly on the temperature. From an extrapolation to the perfect orientation state ($s = 1$), the O–DPDA–O moiety was found to have a potential to afford a huge birefringence of 0.9, which will be useful for optical phase difference films, laser

Published on 15 March 2012. Downloaded by McMaster University on 29/10/2014 16:02:58.

emission films and optical rotation plates. Research is ongoing on applications to high-birefringence films by preparing side-chain-type polymers with the O–DPDA–O moiety incorporated in the side chain.

Notes and references

1 B. Grant, *Mol. Cryst. Liq. Cryst.*, 1978, **48**, 175.
2 B. Grant, N. J. Cleak and R. J. Cox, *Mol. Cryst. Liq. Cryst.*, 1979, **51**, 209.
3 Y. Ozcayir, J. Asrar and A. Blumstein, *Mol. Cryst. Liq. Cryst.*, 1984, **110**, 263.
4 H. Takatsu, K. Takeuchi, Y. Tanaka and M. Sasaki, *Mol. Cryst. Liq. Cryst.*, 1986, **141**, 279.
5 S.-T. Wu and L. R. Dalton, *J. Appl. Phys.*, 1989, **65**, 4372.
6 S.-T. Wu, H. B. Meng and L. R. Dalton, *J. Appl. Phys.*, 1991, **70**, 3013.
7 S.-T. Wu, M. E. Neubert, S. S. Keast, D. G. Abdallah, S. N. Lee, M. E. Walsh and T. A. Dorschner, *Appl. Phys. Lett.*, 2000, **77**, 14.
8 C. S. Hsu, K. F. Shu, Y. Y. Chuang and S. T. Wu, *Liq. Cryst.*, 2000, **27**, 283.
9 C. Sekine, K. Fujisawa, K. Iwakura, N. Konya and M. Minami, *Mol. Cryst. Liq. Cryst. Sci. Technol., Sect. A*, 2001, **364**, 711.
10 P.-T. Lin, S.-T. Wu, C.-Y. Chang and C.-S. Hsu, *Mol. Cryst. Liq. Cryst.*, 2004, **411**, 243.
11 S. Gauza, C.-H. Wen, S.-T. Wu, N. Janarthanani and C.-S. Hsu, *Jpn. J. Appl. Phys.*, 2004, **43**, 7634.
12 Y.-M. Liao, H.-L. Chen, C.-S. Hsu, S. Gauza and S.-T. Wu, *Liq. Cryst.*, 2007, **34**, 507.
13 M. Uchimura, S. Kang, R. Ishige, J. Watanabe and G. Konishi, *Chem. Lett.*, 2010, **39**, 515.
14 A. J. Seed, K. J. Toyne, J. W. Goodby and M. Hird, *J. Mater. Chem.*, 2000, **10**, 2069.
15 G. J. Cross, A. J. Seed, K. J. Toyne, J. W. Goodby, M. Hird and M. C. Artal, *J. Mater. Chem.*, 2000, **10**, 1555.
16 M. E. Neubert, M. R. Fisch, S. S. Keast, J. M. Kim, M. C. Lohman, R. S. Murray, K. J. Miller, R. A. Shenoy, M. J. Smith, R. M. Stayshich, M. E. Walsh, R. G. Petschek, G. A. Lorenzo, D. C. Burrows and S. M. Oliver, *Liq. Cryst.*, 2004, **31**, 941.
17 M. E. Neubert, S. S. Keast, J. M. Kim, K. J. Miller, R. M. Murray, A. G. Norton, R. A. Shenoy, M. E. Walsh and R. G. Petschek, *Liq. Cryst.*, 2004, **31**, 175.
18 R. A. Shenoy, M. E. Neubert, D. G. Abdallah, S. S. Keast and R. G. Petschek, *Liq. Cryst.*, 2000, **27**, 801.
19 M. E. Neubert, S. S. Keast, E. E. Humeniuk, M. E. Walsh and R. G. Petschek, *Liq. Cryst.*, 1999, **26**, 1695.
20 C. M. Hudson, R. A. Shenoy, M. E. Neubert and R. G. Petschek, *Liq. Cryst.*, 1999, **26**, 241.
21 M. Yoshida, T. Doi, S. M. Kang, J. Watanabe and T. Takahashi, *Chem. Commun.*, 2009, 2756–2758.
22 B. Happ, D. Escudero, M. D. Hager, C. Friebe, A. Winter, H. Görls, E. Altuntas, L. González and U. S. Schubert, *J. Org. Chem.*, 2010, **75**, 4025–4038.
23 N. Tanaka, M. Kimura and T. Akahane, *Jpn. J. Appl. Phys.*, 2003, **42**, 486–491.
24 M. Hird, A. J. Seed, K. J. Toyne, J. W. Goodby, G. W. Gray and D. G. McDonnell, *J. Mater. Chem.*, 1993, **3**, 851.
25 S.-T. Wu, H. B. Meng and L. R. Dalton, *J. Appl. Phys.*, 1991, **70**, 15.
26 I. Haller, *Prog. Solid State Chem.*, 1975, **10**, 103.

This journal is © The Royal Society of Chemistry 2012